ELSEVIER

Available online at www.sciencedirect.com

SCIENCE DIRECT®

Nuclear Instruments and Methods in Physics Research B 203 (2003) 183–191

NIM B Beam Interactions with Materials & Atoms

www.elsevier.com/locate/nimb

Potential sputtering of protons from hydrogen- and H_2O-terminated Si(1 0 0) surfaces with slow highly charged ions

K. Kuroki [a,b], K. Komaki [a], Y. Yamazaki [a,c,*]

[a] Institute of Physics, Graduate School of Arts and Sciences, University of Tokyo, 3-8-1 Komaba, Meguro-ku, Tokyo 153-8902, Japan

[b] NRIPS, 6-3-1 Kashiwanoha, Kashiwa, Chiba 277-0882, Japan

[c] RIKEN, 2-1 Hirosawa, Wako, Saitama 351-0198, Japan

Abstract

A potential sputtering mechanism of hydrogen has been studied for impacts of slow highly charged Xe^{q+} ions (<5 keV, $q = 4$–12) on well-defined H-terminated and water-saturated Si(1 0 0) surfaces. It was found that the sputtering yields of protons were proportional to q^{γ} ($\gamma \sim 5$) for both the Si(1 0 0)2 × 1-H and Si(1 0 0)1 × 1-H surfaces, although the absolute yield for the Si(1 0 0)1 × 1-H surface was 10 times larger than that for the Si(1 0 0)2 × 1-H surface, i.e. the sputtering efficiency per one H–Si bond for the Si(1 0 0)1 × 1-H surface is five times larger that for the Si(1 0 0)2 × 1-H surface. The proton sputtering efficiency from a H–O–Si bond was extracted from measurements of the water-saturated surface, which was ~8 times larger than the H–Si bond of the Si(1 0 0)2 × 1-H surface. An effective distance of the proton from its substrate was proposed to be the key parameter to govern the yield, which also influences the energy distributions of sputtered protons. These findings are consistently explained with a pair-wise bond-breaking model induced by a double electron capture, where the classical over barrier process plays an essential role.

© 2003 Elsevier Science B.V. All rights reserved.

PACS: 79.20.Rf

Keywords: Potential sputtering; Highly charged ions; H-terminated Si surface; H_2O-saturated Si surface

1. Introduction

In the last two decades, interactions of slow highly charged ions (HCIs) with various surfaces have been intensively studied because of their exotic nature in collision dynamics, which include multiple electron transfers under strong electric field, formation of hollow atoms (ions), and deposition of large potential energies [1–8]. Further, possible application of slow HCIs to highly-sensitive surface analysis and surface modification are another important aspects that enhance the high activities [9–12].

When a slow HCI bombards a solid surface, atoms and molecules on the surface are emitted as the results of the multiple electron transfers and

* Corresponding author. Tel.: +81-48-467-9482/81-3-5454-6521; fax: +81-48-467-4644/81-3-5454-6433.

E-mail address: yasunori@phys.c.u-tokyo.ac.jp (Y. Yamazaki).

0168-583X/03/$ - see front matter © 2003 Elsevier Science B.V. All rights reserved.
doi:10.1016/S0168-583X(02)02215-2

the localized potential energy deposition, which is called a potential sputtering. In this case, the kinetic energy of the incident HCI does not play any important roles, and can be made small enough so that the radiation damage to the target substrate is negligible. This is compared with a kinetic sputtering, which is induced through a kinetic energy transfer from energetic ions. Although the kinetic sputtering has been adopted as one of the most popular techniques of surface elemental analysis, radiation damage to the substrate is unavoidable, and could also change material properties seriously. In this respect, the potential sputtering with slow HCIs has two extreme advantages, i.e. high sensitivity and low damage, which are usually incompatible. In the present report, we will primarily concentrate on the potential sputtering of protons from hydrogen- and water-terminated Si(1 0 0) surfaces.

Our previous observation of the proton sputtering from untreated surfaces revealed that (1) the sputtering yields were proportional to q^{γ} ($\gamma \sim 5$) for $q < 10$, where q is the charge of the incident HCI, (2) the energy distribution of the sputtered protons was highly non-thermal with a peak at several eV independent of the kinetic energy of the HCI, (3) the sputtering yields level off for kinetic energies lower than several hundreds eV in the case of Ar ions, i.e. the proton sputtering is not induced with the kinetic energy transfer from the HCI but is induced purely with the potential energy [9,13,14]. Similar findings were also reported for HCIs of higher kinetic energies bombarding untreated surfaces, where the observed q-dependences were milder than the above (e.g. $\gamma \sim 4$ for 4.8 keV Ar^{q+} [9] and $\gamma \sim 3$ for 18 keV Ar^{q+} [15]). Such a strong q-dependence in proton sputtering was successfully explained with a pair-wise potential sputtering mechanism based on the classical over barrier model [16].

Recently, a similar research but with hydrogen-terminated Si(1 0 0) surfaces was made [12], which revealed that the charge state dependences were just the same as those of untreated surfaces although the absolute yields depended very much on the surface conditions. In the present report, proton sputtering phenomena from well-defined H_2O-saturated Si(1 0 0) surface are discussed together with the results for the hydrogen terminated Si(1 0 0) surfaces.

2. Pair-wise potential sputtering model

A generally accepted scenario of the interaction of a slow HCI with a conductive surface consists of three steps, i.e. (1) image acceleration of the HCI toward the surface, (2) resonant neutralization of the HCI above the surface via the classical over barrier process and (3) release of the potential energy at or slightly below the surface [6]. Viewing the above scenario from the target side, these processes are read as (1) accumulation of valence electrons near the surface (polarization), (2) multiple electron removal from a localized area of the surface in a short time, which causes a temporary charge up and (3) high-density energy deposition. The collision system discussed in the present paper could also be handled with the same manner except for the fact that an insulating layer of hydrogen or dissociated water molecule covers the conductive substrate. It is evident that the step (2) and/or the step (3) play an important role in the secondary ion emission with slow HCIs. One of the promising mechanisms to explain the observation is schematically shown in Fig. 1 taking Si–H bonds as an example [17]: When an HCI approaches one of chemical bonds on the surface, electrons in the bond are sequentially transferred to the HCI, resulting in mutual Coulomb repulsion among charged species, and eventually, an ionized atom is released from the bond, which is called a pair-wise potential sputtering. [1] Whenever an electron is transferred from the bond to the HCI, it forms a temporal molecular orbital and is shared by the bond and the HCI. The probability of the electron in the HCI orbit for a specific Si–H bond may be determined by the ratio of the phase space volume, which is n^2:1, where n is the principal

[1] Although the mechanism was named "potential sputtering", the sputtering considered here is induced not with the potential energy deposition but with a mutual Coulomb repulsion induced with multiple resonant charge transfer, where the energy release does not play important roles.

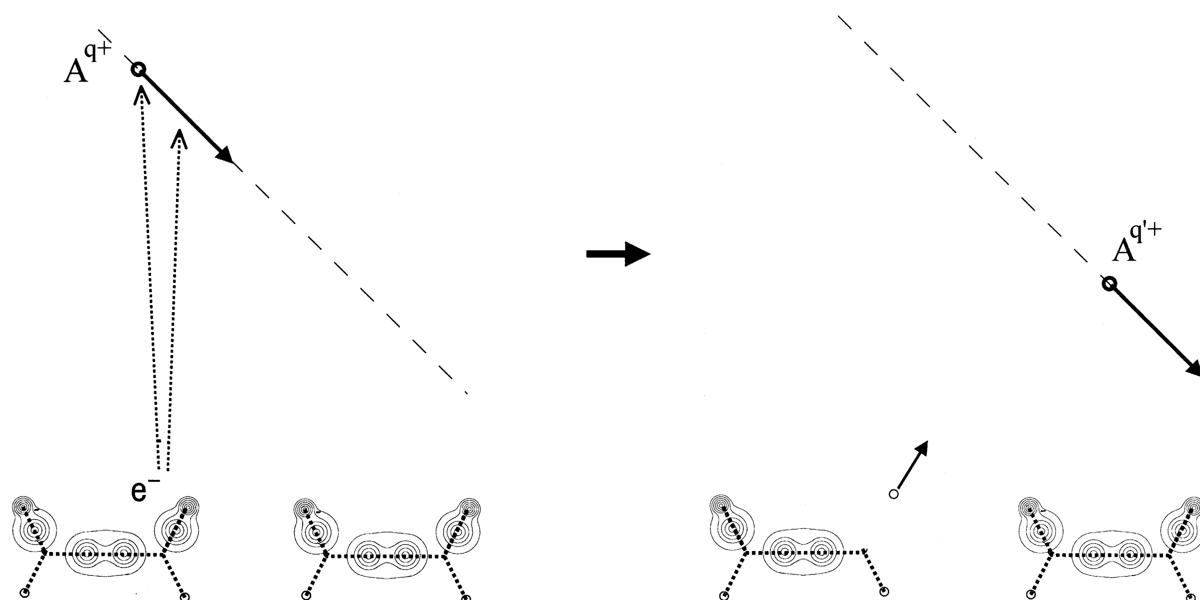

Fig. 1. A Schematic diagram showing the potential sputtering of hydrogen with an HCI from the Si–H bond of the Si(1 0 0)2 × 1-H surface (see Fig. 6(a)). The contour lines show the electron distributions of H—Si=Si—H bonds [17].

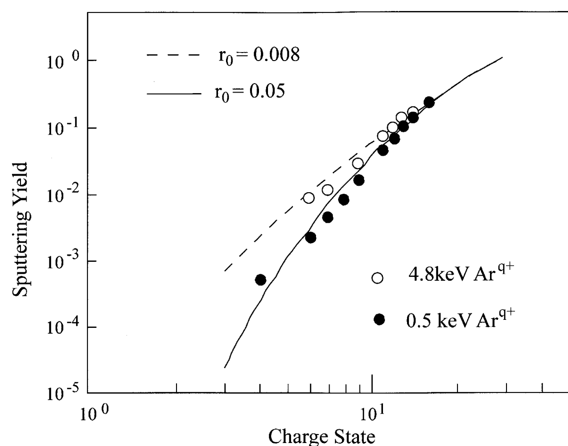

Fig. 2. The proton sputtering yield from untreated surfaces as a function of incident charge q. Experimental data: ● at 500 eV Ar^{q+}; ○ at 4.8 keV Ar^{q+} [16].

quantum number of the electronic state of the transferred electron. Considering that $n \sim q$ [6], the probability for the hydrogen to remain charged escaping from the reneutralization is proportional to q^2. Crudely speaking, two-electron transfer from the same bond is a minimum requirement to induce effective ion emission, and the secondary ion yields induced with slow HCIs are expected to be proportional to q^4 or even stronger. Such a process should become effective when the bond is non-conductive because the Coulomb repulsion lasts for a finite time till electrons in the substrate reneutralize the bond. The predicted sputtering yields are shown in Fig. 2, which successfully reproduced the strong charge state dependence [16].

3. Experimental

Fig. 3 shows a schematic diagram of the experimental setup used to study the potential sputtering from well-defined surfaces. A slow HCI beam extracted from the electron beam ion source (EBIS) [18] was charge-state selected with the Wien filter, chopped by the deflector to make a short pulse train of 40 ns–2 μs wide with a repetition rate of 50 kHz, and then was introduced in the collision chamber through the 1.5 mm aperture [19].

At the center of the collision chamber, a target holder was mounted on a linear and rotation feedthrough. A ceramic heater was on the holder, which was used to prepare the reconstructed

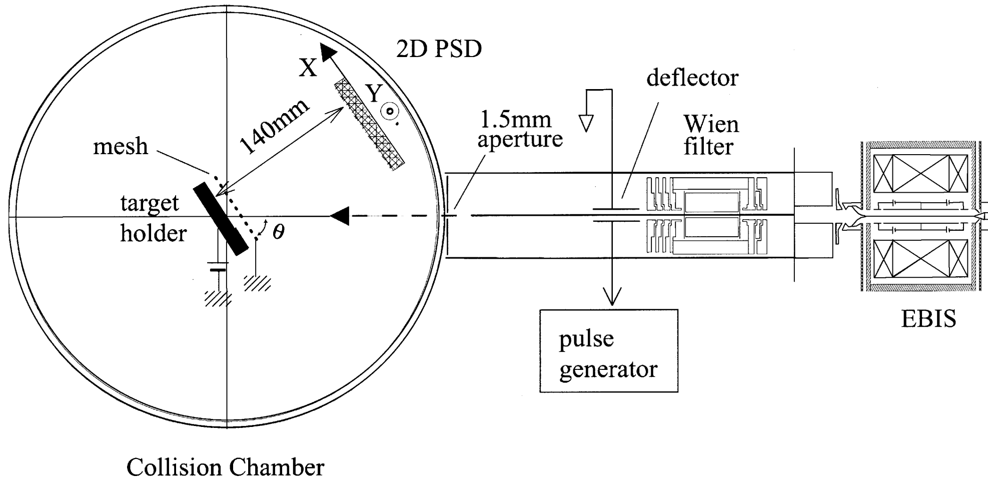

Fig. 3. A schematic diagram of the experimental setup [19].

Si(1 0 0)2 × 1 clean surface. The Si(1 0 0)2 × 1-H surface was obtained by exposing the clean Si(1 0 0)2 × 1 surface to atomic hydrogen keeping the substrate temperature at 600 K until the coverage saturated. The Si(1 0 0)3 × 1-H and Si(1 0 0)1 × 1-H surfaces were prepared by exposing the Si(1 0 0)2 × 1-H surface further to atomic hydrogen at 400 K and at room temperature, respectively. The procedure to prepare the Si(1 0 0)3 × 1-H and Si(1 0 0)1 × 1-H surfaces via the Si(1 0 0)2 × 1-H surface was found to be very useful to make consistent experiments because the clean Si(1 0 0)2 × 1 surface is quite active and unstable against a tiny amount of water molecules. Further details of the sample treatment can be found elsewhere [12,19].

A gold plated W-mesh at the ground potential was prepared at $d_1 = 11$ mm above the target surface, which was biased to extract positively charge secondary ions. The uniform electric field formed between the target and the W-mesh was used to accelerate secondary ions toward the two-dimensional position sensitive detector (2DPSD) located at $d_2 = 140$ mm from the target [19,20]. When a singly charged ion is detected at x mm from the center of the 2DPSD, which is defined by the position hit by a particle with zero transverse energy, the transverse energy ε_t of the ion is given by

$$\varepsilon_t(\mathrm{eV}) = x^2/(d_1 + d_2)^2 V, \quad (1)$$

where V is the bias of the target. The base pressure of the collision chamber was 3×10^{-10} Torr.

4. H-terminated surfaces

Fig. 4(a) shows an example of the TOF spectrum of secondary ions when 3 keV Xe^{8+} ions were injected upon the Si(1 0 0)2 × 1-H surface at $\theta = 24°$. The major components were proton, Si^+, Si_2^+ and $Si_2OH_n^+$ ($n = 0$–2) ions. Weak bumps of Si_n^+ ($n = 3, 4$) ions were also observed. On the other hand, $SiO(H)^+$ ions were barely seen (cf. Fig. 7(a)). The Si^+ peak skewed to the shorter TOF side, which corresponds to the longitudinal kinetic energy $\varepsilon_l(Si^+; 2 \times 1)$ of several eV.

Fig. 4(b) shows the 2D distribution of sputtered protons for the target bias of 325 V, which is relatively narrow and is more or less isotropic. Using Eq. (1), an average transverse energy of the proton emitted from the Si(1 0 0)2 × 1-H surface $\varepsilon_t(p; 2 \times 1)$ was estimated to be ~0.25 eV. On the other hand, $\varepsilon_t(p; 1 \times 1)$ was ~1 eV, i.e. ε_t depends very strongly on the surface condition [12,19].

Fig. 4(c) shows that the Si^+ ions were emitted non-uniformly with a preference toward the downstream side of the HCI. $\varepsilon_t(Si^+; 2 \times 1)$ is seen to be comparable to $\varepsilon_l(Si^+; 2 \times 1)$. The 2D

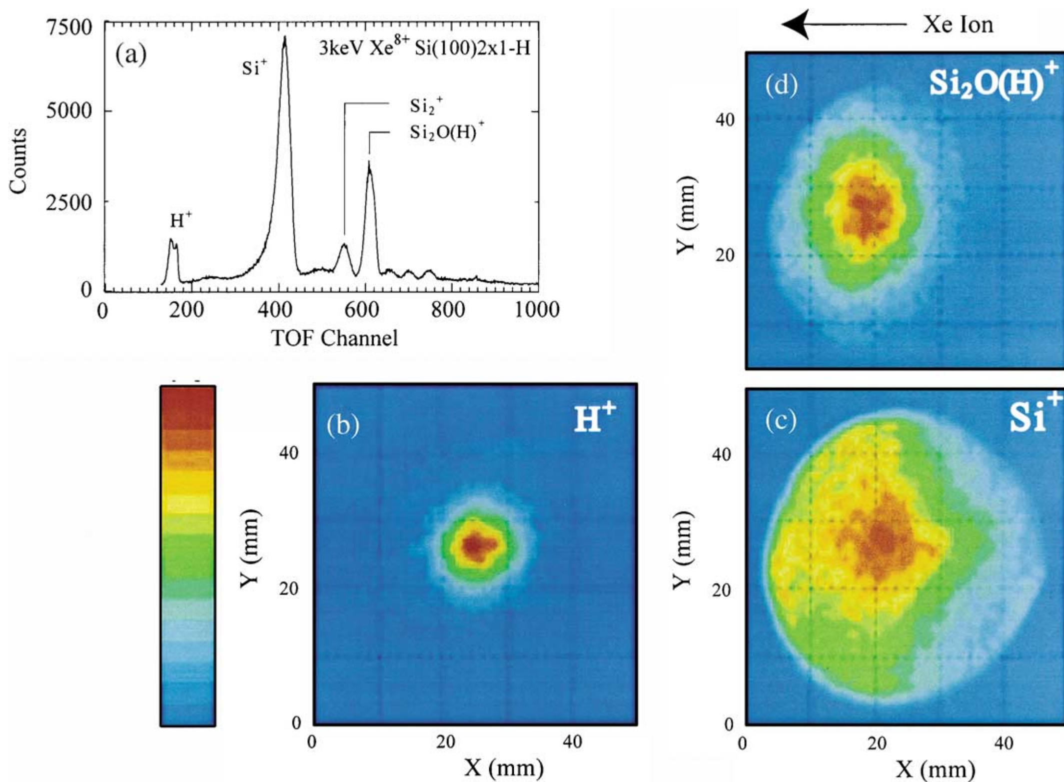

Fig. 4. (a) An example of the TOF spectrum for 3 keV Xe^{8+} impacts on the Si(1 0 0)2 × 1-H surface with the target bias of 325 V. The 2D distributions of (b) proton, (c) Si^+ and (d) $Si_2O(H)^+$ ions.

distribution of the $Si_2O(H)^+$ ions (Fig. 4(d)) was elliptic with its long axis perpendicular to the HCI direction. It is also noted that the center of the proton distribution appeared about 5 mm upstream from those of the other two species, indicating that the trajectories of the outgoing protons might be influenced by the electric field of the HCI when it was above the surface (see Fig. 1) [20].

Fig. 5 shows the sputtering yields of protons and Si^+ ions from the Si(1 0 0)2 × 1-H and Si(1 0 0)1 × 1-H surfaces bombarded with Xe^{q+} ions as a function of q. The dashed lines show the q^5 dependences, which more or less reproduce the observations for both Si(1 0 0)2 × 1-H and Si(1 0 0)1 × 1-H surfaces. As discussed in Section 2, this strong q dependence looks universal independent of the details of the surface condition [9,13,14]. It was also found that the sputtering yields of proton did not depend on the incident angle of the HCI [12] although the Si^+ sputtering yield showed a strong dependence on the incident angle, which is a specific feature to the kinetic sputtering [21].

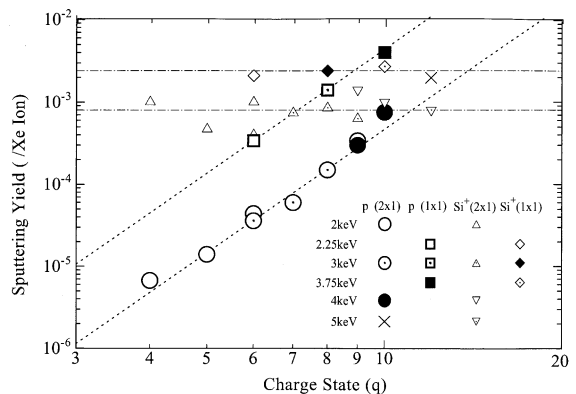

Fig. 5. Sputtering yield of proton and Si^+ from Si(1 0 0)2 × 1-H and Si(1 0 0)1 × 1-H surfaces as a function of q. The dashed lines show q^5 dependence. The energy values are for the primary Xe^{q+} ions [12].

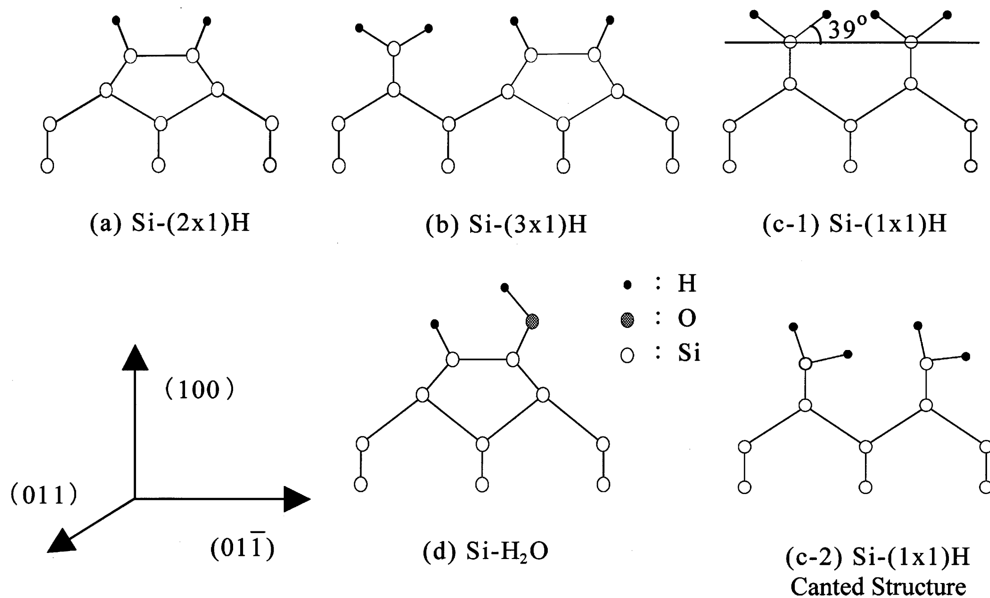

Fig. 6. Surface structures of (a) Si(1 0 0)2 × 1-H, (b) Si(1 0 0)3 × 1-H, (c–1) Si(1 0 0)1 × 1-H (symmetry), (c–2) Si(1 0 0)1 × 1-H (canted) and (d) Si(1 0 0)2 × 1-H_2O.

The absolute proton sputtering yields from the Si(1 0 0)2 × 1-H, Si(1 0 0)3 × 1-H and Si(1 0 0)11-H surfaces bombarded with 3 keV Xe^{8+} ions were $\sim 1.2 \times 10^{-4}$/ion, $\sim 2.0 \times 10^{-4}$/ion and $\sim 1.3 \times 10^{-3}$/ion, respectively. TDS measurements showed that the coverages of hydrogen for these surfaces were 1, 1.5 and 2.0 monolayer (ML), respectively, i.e. the proton yield for the Si(1 0 0)1 × 1-H surface normalized per Si–H bond was ~5 times larger than the other two. This large enhancement can be attributed to the fact that (1) the Si(1 0 0)1 × 1-H surface is atomically rough while the Si(1 0 0)2 × 1-H and Si(1 0 0)3 × 1-H surfaces are atomically flat [22], and/or (2) the Si(1 0 0)1 × 1-H surface may take a so-called canted structure (Fig. 6(c–2)) instead of a symmetric structure (Fig. 6(c–1)). For both cases, an effective distance of the hydrogen from the substrate is larger than, e.g. that of the Si(1 0 0)2 × 1-H case (Fig. 6(a)). It is easy to imagine that an ion in the bond on an atomically rough surface is less likely to be reneutralized as compared with that on an atomically flat surface. Further, reneutralization of Si^+ ion may also be slower for a rough surface, leading to a prediction that the emission energy of proton has a positive correlation with the sputtering yield, which has actually been confirmed among the three different Si(1 0 0) surfaces and untreated surfaces [12]. It is noted that the 2D distributions consist only of a single peak at the center, which is not in accord with a naive expectation that the angular distribution of sputtered protons reflects (1) the direction of the Si–H bond before sputtering and (2) the repulsion from the HCI.

Fig. 5 shows that the Si^+ sputtering yields stayed constant over the charge states studied although the absolute values were different between the two surfaces, 2.3×10^{-3} and 8×10^{-4} for the Si(1 0 0)1 × 1-H and the Si(1 0 0)2 × 1-H surfaces, respectively. For both protons and Si^+ ions, the sputtering yields for the Si(1 0 0)1 × 1-H surface were larger than those for the Si(1 0 0)2 × 1-H surface. Considering that the total sputtering yield of Si for 3 keV Xe^+ is about 1.5 atoms/ion [23], the charged fraction is ~0.1%.

5. Sputtering from the water-saturated Si(1 0 0)2 × 1 surface

As has been discussed in Section 4, both the proton sputtering yields and the emission energy

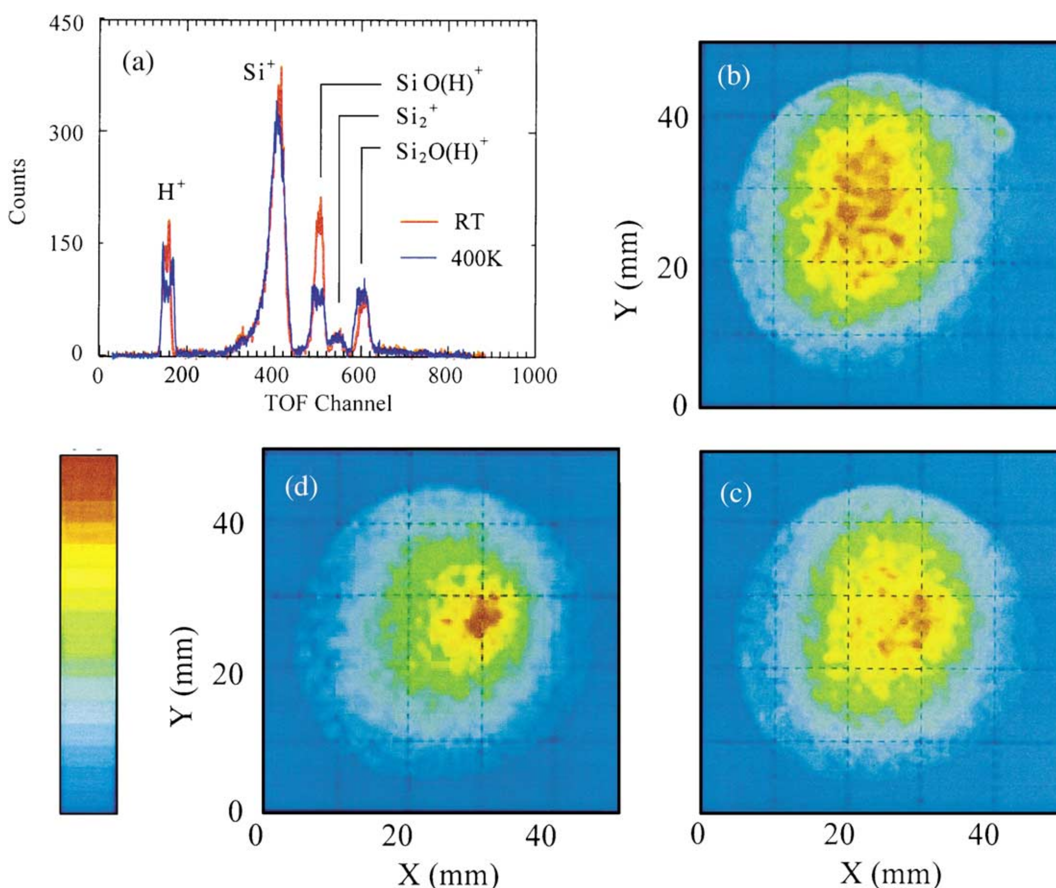

Fig. 7. (a) An example of the TOF spectrum for 3 keV Xe^{8+} impacts on the water-saturated Si(1 0 0)2 × 1 surface with the target bias of 325 V. The red and blue curves are for the target at the room temperature and at 400 K, respectively. The 2D distributions of protons at (b) the room temperature, (c) 400 K for 1 h and (d) 400 K after 24 h.

increase drastically as an effective distance of the emitter from the substrate gets larger. In order to see whether this idea is extendable, the water-saturated Si(1 0 0)2 × 1 surface (referred to as the Si(1 0 0)2 × 1H_2O surface, hereafter) was adopted. It is known that a water molecule is dissociatively adsorbed on the Si(1 0 0) surface at the room temperature forming Si–H and Si–OH bonds keeping the surface atomically flat [24]. A schematic structure of the Si(1 0 0)2 × 1-H_2O surface is shown in Fig. 6(d). It is seen that the hydrogen on the Si–O–H bond is away from the substrate and the sputtering yield is expected to be large. The amount of adsorbed water molecule was evaluated by observing the amount of desorbed H_2 with the TDS method. It was found that the amount of hydrogen on the Si(1 0 0)2 × 1-H_2O surface was ~76% of that on the Si(1 0 0)1 × 2-H surface, i.e. 0.38 ML of water was adsorbed, which is consistent with published data [25].

The red curve in Fig. 7(a) shows the TOF spectrum of secondary ions when the Si(1 0 0)2 × 1-H_2O surface was bombarded with 3 keV Xe^{8+} ions. In contrast to H-terminated surfaces (see Fig. 4(a)), the $SiO(H)^+$ ion yield grew considerably, and at the same time, other peaks consisting purely of Si atoms were much suppressed. The proton yield for 3 keV Xe^{8+} ions was 4.2×10^{-4}. Considering that the saturated coverage is 76%, and comparing the yield with that of the Si(1 0 0)2 × 1-H

surface, one can estimate a relative proton yield from the Si–OH bond to that from the Si–H bond, which is $(4.2 \times 10^{-4}/0.38 - 1.2 \times 10^{-4})/1.2 \times 10^{-4} \sim 8.2$, which is just what is speculated in the above paragraph.

It is known that the OH bond on the Si(1 0 0)2 × 1-H_2O surface disappears when the surface is heated at around 620 K [26]. In order to see the sensitivity of our method, the TOF spectrum and the 2D distribution were measured keeping the sample at 400 K for 24 h. The blue curve in Fig. 7(a) shows the TOF spectrum. The intensities of the proton and $SiO(H)^+$ peaks became ~60% and ~45% of those of the red curves, respectively. If the $SiO(H)^+$ intensity is proportional to the number of remaining OH bonds, the proton yield is expected to become 57% employing the enhancement factor of 8.2, which is consistent with the observed reduction to ~60%.

The 2D distributions of the sputtered protons from the Si(1 0 0)2 × 1-H_2O surface kept at the room temperature, at 400 K for 1 h, and at 400 K after 24 h are shown in Figs. 7(b) and (c) and 6(d), respectively. It is interesting to see that the elliptic distribution observed at the room temperature got more uniform immediately after the target temperature was raised to 400 K, which became a narrow spot after 24 h, which looks similar to the distribution of the Si(1 0 0)2 × 1-H surface (see Fig. 4(b)). These observations are consistent with previous observations that the OH bonds disappear when the target temperature is raised to 620 K. It is noted that the present technique is very sensitive to the change of the surface structure which takes place even at 400 K.

6. Summary

Proton sputtering phenomena with slow HCIs were studied for four different well-defined Si(1 0 0) surfaces. The proton sputtering yields for the Si(1 0 0)2 × 1-H and Si(1 0 0)1 × 1-H surfaces were proportional to q^γ ($\gamma \sim 5$) like in the case of untreated surfaces, indicating that this feature is rather universal to the proton sputtering with slow HCIs. The proton sputtering yields for the Si(1 0 0)2 × 1-H, Si(1 0 0)3 × 1-H, Si(1 0 0)1 × 1-H, and water-saturated Si(1 0 0)2 × 1 surfaces bombarded with 3 keV Xe^{8+} ions were $\sim 1.2 \times 10^{-4}$/ion, $\sim 2.0 \times 10^{-4}$/ion, and $\sim 1.3 \times 10^{-3}$/ion, and 4.2×10^{-4}/ion, respectively. The kinetic energies of sputtered protons had positive correlation with the sputtering yields. These observations were consistent with the prediction of the pair-wise potential sputtering model taking into account a reneutralization process based on the over barrier model although the quantitative understanding on the angular distributions is left as an interesting future problem.

References

[1] J.P. Briand, L. de Billy, P. Charles, S. Essabaa, P. Briand, R. Geller, J.P. Desclaux, S. Bliman, C. Ristori, Phys. Rev. Lett. 65 (1990) 159.
[2] H. Winter, Europhys. Lett. 18 (1992) 207.
[3] H. Kurtz et al., Phys. Rev. Lett. 69 (1992) 1140.
[4] J. Das, R. Morgenstern, Phys. Rev. A 47 (1993) R755.
[5] M. Grether, A. Spieler, R. Köhrbrück, N. Stolterfort, Phys. Rev. A 52 (1995) 426.
[6] J. Burgdörfer, P. Lerner, F.W. Meyer, Phys. Rev. A 44 (1991) 5674.
[7] S. Ninomiya, Y. Yamazaki, F. Koike, H. Masuda, T. Azuma, K. Komaki, K. Kuroki, M. Sekiguchi, Phys. Rev. Lett. 78 (1997) 4557.
[8] T. Schenkel, A.V. Barnes, T.R. Niedermayr, M. Hattass, M.W. Newman, G.A. Machicoane, J.W. McDonald, A.V. Hamza, D.H. Schneider, Phys. Rev. Lett. 83 (1999) 4273.
[9] N. Kakutani, T. Azuma, Y. Yamazaki, K. Komaki, K. Kuroki, Jpn. J. Appl. Phys. 34 (1995) L580.
[10] A.V. Hamza et al., Appl. Phys. Lett. 79 (2001) 2973.
[11] G. Hayderer et al., Phys. Rev. Lett. 86 (2001) 3530.
[12] K. Kuroki, N. Okabayashi, H. Torii, K. Komaki, Y. Yamazaki, Appl. Phys. Lett. 81 (2002) 3561.
[13] N. Kakutani, T. Azuma, Y. Yamazaki, K. Komaki, K. Kuroki, Nucl. Instr. and Meth. B 96 (1995) 541.
[14] K. Kuroki, T. Takahira, Y. Tsuruta, N. Okabayashi, T. Azuma, K. Komaki, Y. Yamazaki, Phys. Scr. T 80 (1999) 557.
[15] S. Della-Negra, J. Depauw, H. Joret, V. Le Beyec, E.A. Schweikert, Phys. Rev. Lett. 60 (1988) 948.
[16] J. Burgdörfer, Y. Yamazaki, Phys. Rev. A 54 (1996) 4140.
[17] C.J. Wu, E.A. Carter, Chem. Phys. Lett. 185 (1991) 172.
[18] K. Okuno, Jpn. J. Appl. Phys. 28 (1989) 1124.
[19] K. Kuroki, N. Okabayashi, H. Torii, K. Komaki, Y. Yamazaki, Nucl. Instr. and Meth. B 193 (2002) 804.
[20] N. Okabayashi, K. Kuroki, Y. Tsuruta, T. Azuma, K. Komaki, Y. Yamazaki, Phys. Scr. T 80 (1999) 555.

[21] P. Sigmund, Phys. Rev. 184 (1969) 383.
[22] J.J. Boland, Phys. Rev. Lett. 65 (1990) 3325.
[23] N. Matsunami, Y. Yamamura, Y. Itikawa, N. Itoh, Y. Kazumata, S. Miyagawa, K. Morita, R. Shimizu, H. Tawara, Atomic Data Nucl. Data 31 (1984) 1.
[24] L. Andersohn, U. Kohler, Surf. Sci. 77 (1993) 284.
[25] M.C. Flowers, B.B.H. Jonathan, A. Morris, S. Wright, Surf. Sci. 351 (1996) 87.
[26] X.L. Zhou, C.R. Flores, J.M. White, Appl. Surf. Sci. 62 (1992) 223.